13th World Conference on Earthquake Engineering
Vancouver, B.C., Canada
August 1-6, 2004
Paper No. 843

NON-LINEAR SEISMIC ANALYSIS OF MASONRY STRUCTURES

Alessandro GALASCO[1], Sergio LAGOMARSINO[2], Andrea PENNA[3] and Sonia RESEMINI[4]

SUMMARY

Complete 3D models of URM structures can be obtained assembling 2-nodes macro-elements, representing the non-linear behaviour of masonry panels and piers. This modelling strategy has been implemented in the TREMURI program with non-linear static and dynamic analysis procedures requiring limited computational loads. By means of internal variables, the macro-element considers both the shear-sliding damage failure mode and its evolution, controlling the strength deterioration and the stiffness degradation, and rocking mechanisms, with toe crushing effect. URM building models can be obtained assembling plane structures, walls and floors. Masonry arch bridges can be modelled and analysed through the macro-element approach, too.

INTRODUCTION

The need for masonry structure modelling and analysis tools is largely diffused worldwide. Very sophisticated finite element models or extremely simplified methods are commonly used for the seismic analysis of this kind of structures. In this paper, by means of the effective macro-element approach, an accurate, but without heavy computational load, modelling strategy is presented and developed for the analysis of both building and bridge structures.
Case studies and examples, both from experimental testing and earthquake damaged structures, show the modelling technique effectiveness and the seismic analysis capabilities. Pushover analyses provide capacity curves and equivalent hysteretic damping evaluation: these results permit to assess the applicability of the Capacity Spectrum Method to masonry structures, checking the seismic performance prediction by dynamic analyses.

NON-LINEAR MACRO-ELEMENT MODELLING

The non-linear macro-element model, representative of a whole masonry panel, proposed by Gambarotta [1], permits, with a limited number of degrees of freedom (8), to represent the two main in-plane masonry failure modes, bending-rocking and shear-sliding (with friction) mechanisms, on the basis of mechanical

[1] PhD Student, Department of Structural and Geotechnical Engineering, University of Genoa, Italy
[2] Professor, Department of Structural and Geotechnical Engineering, University of Genoa, Italy
[3] Researcher, European Centre for Training and Research in Earthquake Engineering, Pavia, Italy
[4] Research Assistant, Department of Structural and Geotechnical Engineering, University of Genoa, Italy

assumptions. This model considers, by means of internal variables, the shear-sliding damage evolution, which controls the strength deterioration (softening) and the stiffness degradation.
Figure 1 shows the three sub-structures in which a macro element is divided: two layers, inferior ① and superior ③, in which the bending and axial effects are concentrated. Finally, the central part ② suffers shear-deformations and presents no evidence of axial or bending deformations. A complete 2D kinematic model should to take into account the three degrees of freedom for each node "i" and "j" on the extremities: axial displacement w, horizontal displacement u and rotation φ. There are two degrees of freedom for the central zone: axial displacement δ and rotation ϕ (figure 1).

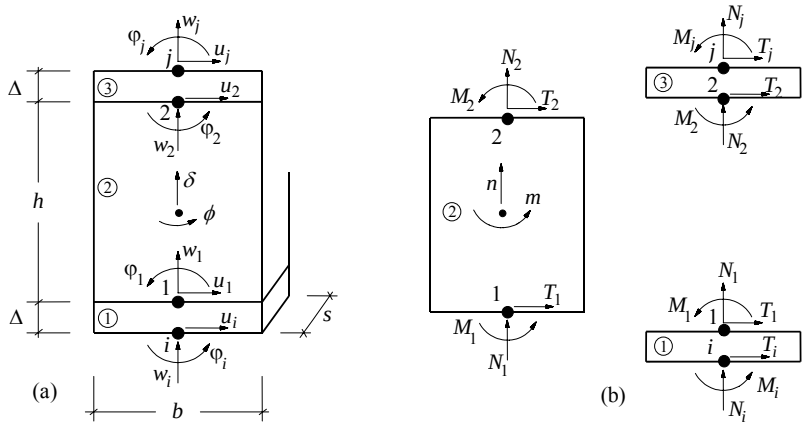

Figure 1. Kinematic model for the macro-element (Gambarotta [1])

Thus, the kinematics is described by an eight degree freedom vector, $a^T = \{u_i\ w_i\ \varphi_i\ u_j\ w_j\ \varphi_j\ \delta\ \phi\}$, which is obtained for each macro-element. It is assumed that the extremities have an infinitesimal thickness ($\Delta \to 0$).
The overturning mechanism, which happens because the material does not show tensile strength, is modeled by a mono-lateral elastic contact between ① and ③ interfaces. The constitutive equations between the kinematic variables w, φ and the correspondent static quantities n and m are uncoupled until the limit condition $\left|\frac{m}{n}\right| \le \frac{b}{6}$, for which the partialization effect begins to develop in the section.
For sub-structure ① the following equations are obtained:

$$N_i = kA(\delta - w_i) + N_i^* \quad , \tag{1}$$

$$M_i = \frac{1}{12} kAb^2(\varphi_i - \phi) + M_i^* \quad , \tag{2}$$

where $A = s \cdot b$ corresponds to the transversal area of the panel. The inelastic contribution N^*_i and M_i^* are obtained from the mono-lateral condition of perfect elastic contact:

$$N_i^* = \frac{-k \cdot A}{8|\varphi_i - \phi|}\left[|\varphi_i - \phi|b + 2(\delta - w_i)\right]^2 H\left(|e_i| - \frac{1}{6}b\right), \tag{3}$$

$$M_i^* = \frac{k \cdot A}{24(\varphi_i - \phi)|\varphi_i - \phi|}\left[(\varphi_i - \phi)b - (\delta - w_i)\right]\left[|\varphi_i - \phi|b + 2(\delta - w_i)\right]^2 H\left(|e_i| - \frac{1}{6}b\right) \quad , \tag{4}$$

where $H(\bullet)$ is the Heaviside function.

The panel shear response is expressed considering a uniform shear deformation distribution $\gamma = \frac{u_i - u_j}{h} + \phi$ in the central part ② and imposing a relationship between the kinematic quantities u_i, u_j and ϕ, and the shear stress $T_i = -T_j$. The cracking damage is usually located on the diagonal, where the displacement take place along the joints and is represented by an inelastic deformation component, which is activated when the Coulomb's limit friction condition is reached. From the effective shear deformation corresponding to module ② and indicating the elastic shear module as *G*, the constitutive equations can be expressed as:

$$T_i = \frac{GA}{h}\left(u_i - u_j + \phi h\right) + T_i^* \quad , \tag{5}$$

$$T_i^* = -\frac{GA}{h}\frac{c\alpha}{1+c\alpha}\left(u_i - u_j + \phi h + \frac{h}{GA} f\right), \tag{6}$$

where the inelastic component T_i^* includes the friction stress f effect, opposed to the sliding mechanism, and involves a damage parameter α and a non-dimensional coefficient c, that controls the inelastic deformation. In this model, the friction plays the role of an internal variable, defined by the following limit condition:

$$\Phi_S = |f| - \mu \cdot N_i \le 0, \tag{7}$$

where μ corresponds to the friction coefficient. These constitutive equations can represent the panel resistance variation due to changes on axial stresses $N_j = -N_i$. The damage effects upon panel mechanical characteristics are described by the damage variable α, that grows according to a pre-defined failure criteria:

$$\Phi_d = Y(S) - R(\alpha) \le 0, \tag{8}$$

where $Y = \frac{1}{2} cq^2$ is the damage energy release rate; *R* is the resistance function and $S = \{t \quad n \quad m\}^{\mathrm{T}}$ is the internal stress vector. Assuming *R* as a growing function of α to the critical value $\alpha_C = 1$ and decreasing for higher values, the model can represent the stiffness degradation, the strength degradation and pinching effect.

The complete constitutive model, for the macro element, can be expressed in the following form:

$$Q = Ka + Q^* \quad , \tag{9}$$

where $Q^* = \left\{T_i^* \; N_i^* \; M_i^* \; T_j^* \; N_j^* \; M_j^* \; N^* \; M^*\right\}$ contains the non-linear terms evaluated by the evolution equations, related to the damage variable α and the friction f, and *K* is the elastic stiffness matrix.

The non-linear terms N^* and M^* are defined through the following equation:

$$N^* = N_j^* - N_i^*; M^* = -M_j^* - M_i^* + T_i^* h \, . \tag{10}$$

The macro-element shear model is a macroscopic representation of a continuous model (Gambarotta [2]), in which the parameters are directly correlated to the mechanical properties of the masonry elements. The macro-element parameters should be considered as representative of an average behaviour. In addition to its geometrical characteristics, the macro-element is defined by six parameters: the shear module *G*, the axial stiffness *K*, the shear strength f_{vq_0} of the masonry, the non-dimensional coefficient c that controls

the inelastic deformation, the global friction coefficient f and the β factor, that controls the softening phase.

Crushing and compressive damage model

The macro-element used in the program to assemble the wall model keeps also into account the effect (especially in bending-rocking mechanisms) of the limited compressive strength of masonry (Penna [3]). Toe crushing effect is modelled by means of phenomenological non-linear constitutive law with stiffness deterioration in compression: the effect of this modellization on the cyclic vertical displacement-rotation interaction is represented in figure 2.

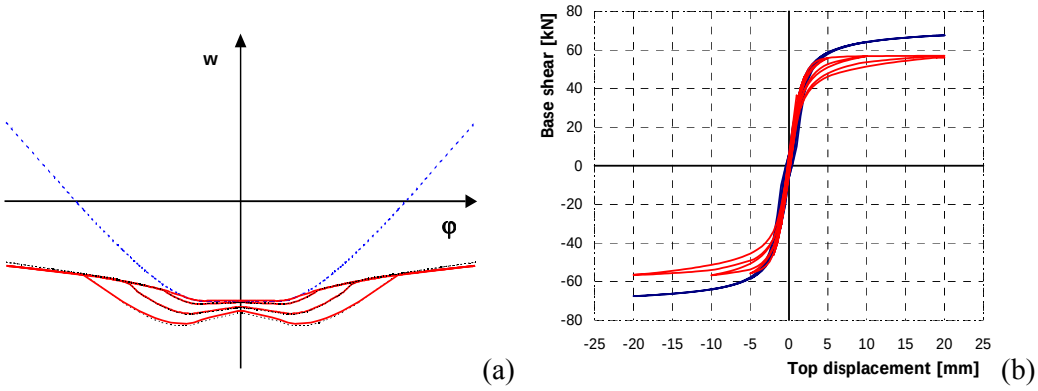

Figure 2. (a) Cyclic vertical displacement-rotation interaction with (red line) and w/o toe crushing (blue dots) in Penna [3]; (b) Rocking panel with (red line) and without (blue line) crushing.

Mono-dimensional non-linear element for 3D modelling

In order to model the masonry bridges, the need for a non-linear element for 3D modelling arose (Resemini [4]). The formulation of this mono-dimensional non-linear element having a truncated-pyramid shape is a 3D extension of the 2D one. Even this element is divided into three portions. In the central part ②, the shear behaviour (with non-linearity, damage and sliding related to frictional effects – in one pre-defined direction) and the torsional behaviour develop. In the two layers, inferior① and superior③, the bending and axial effects (considering partialization and crushing) are modeled.

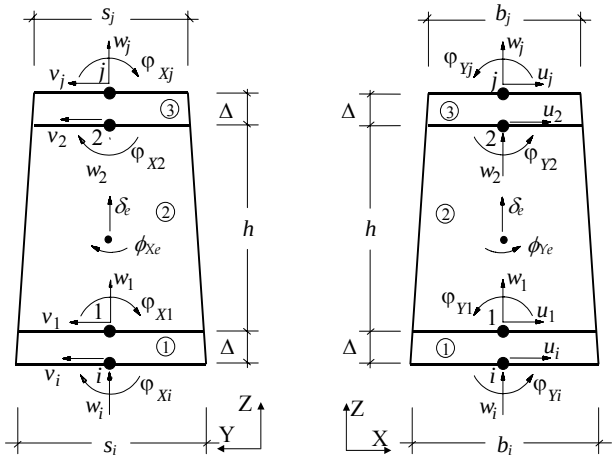

Figure 3. Kinematic model of the element (lateral views) (Resemini [4]).

3D URM BUILDING MODEL

The 3-dimensional modelling of whole URM buildings starts from some hypotheses on their structural and seismic behaviour: the bearing structure, both referring to vertical and horizontal loads, is identified, inside the construction, with walls and floors (or vaults); the walls are the bearing elements, while the floors, apart from sharing vertical loads to the walls, are considered as planar stiffening elements (orthotropic 3-4 nodes membrane elements), on which the horizontal actions distribution between the walls depends; the local flexural behaviour of the floors and the walls out-of-plane response are not computed because they are considered negligible with respect to the global building response, which is governed by their in-plane behaviour (a global seismic response is possible only if vertical and horizontal elements are properly connected).

In-plane behaviour wall model

A frame-type representation of the in-plane behaviour of masonry walls is adopted: each wall of the building is subdivided into piers and lintels (2 nodes macro-elements) connected by rigid areas (nodes). Earthquake damage observation shows, in fact, that only rarely (very irregular geometry or very small openings) cracks appear in these areas of the wall: because of this, the deformation of these regions is assumed to be negligible, relatively to the macro-element non-linear deformations governing the seismic response. The presence of stringcourses (beam elements), tie-rods (non-compressive spar elements), previous damage, heterogeneous masonry portions, gaps and irregularities can be easily included in the structural model.

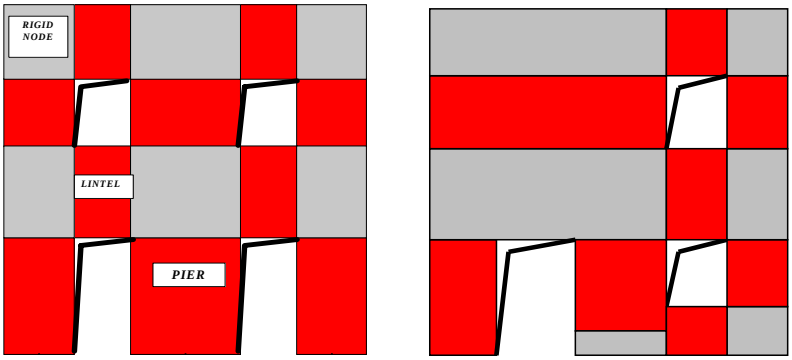

Figure 4. Examples of macro-element modelling of masonry walls.

The non-linear macro-element model, representative of a whole masonry panel, is adopted for the 2-nodes elements representing piers and lintels. Rigid end offsets are used to transfer static and kinematic variables between element ends and nodes.

3D Model

A global Cartesian coordinate system (X,Y,Z) is defined and the wall vertical planes are identified by the coordinates of one point and the angle formed with X axis. In this way, the walls can be modelled as planar frames in the local coordinate system and internal nodes can still be 2-dimensional nodes with 3 d.o.f..

The 3D nodes connecting different walls in corners and intersections need to have 5 d.o.f. in the global coordinate system (u_X, u_Y, u_Z, rot_X, rot_Y): the rotational degree of freedom around vertical Z axis can be neglected because of the membrane behaviour adopted for walls and floors. These nodes can be obtained assembling 2D rigid nodes acting in each wall plane (see figure 5) and projecting the local degrees of freedom along global axes.

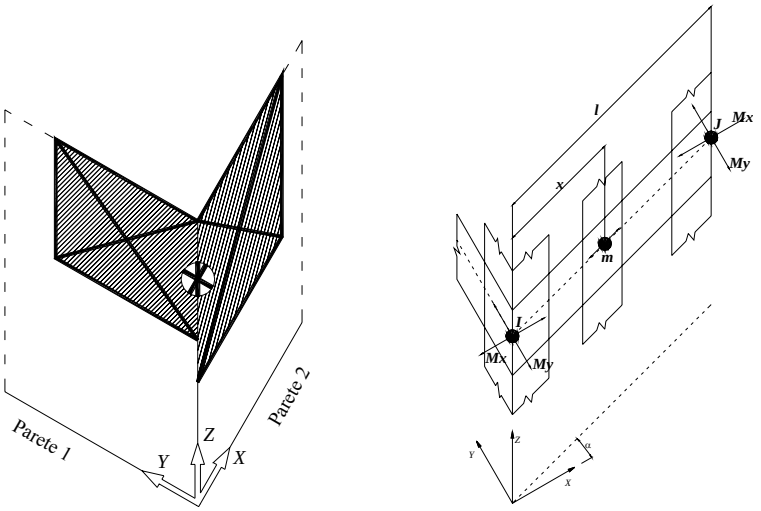

Figure 5. Scheme of 3D and 2D nodes and out-of-plane mass sharing.

The floor elements, modelled as orthotropic membrane finite elements, with 3 or 4 nodes, are identified by a principal direction, with Young modulus E_1, while E_2 is the Young modulus along the perpendicular direction, ν is the Poisson ratio and $G_{1,2}$ the shear modulus: E_1 and E_2 represent the wall connection degree due to the floors, by means also of stringcourses and tie-rods. $G_{1,2}$ represents the in-plane floor shear stiffness which governs the horizontal actions repartition between different walls.
Having the 2D nodes no degrees of freedom along the orthogonal direction to the wall plane, in the calculation the nodal mass component related to out-of-plane degrees of freedom is shared to the corresponding dofs of the nearest 3D nodes of the same wall and floor according to the following relations:

$$\begin{aligned} M_x^I &= M_x^I + m(1-|\cos\alpha|)\frac{l-x}{l} \\ M_y^I &= M_y^I + m(1-|sin\alpha|)\frac{l-x}{l} \end{aligned}, \qquad (11)$$

where the meaning of the terms is shown in figure 5.
This solution then permits the implementation of static analyses with 3 components of acceleration along the 3 principal directions and 3D dynamic analyses with 3 simultaneous input components, too.

3D MASONRY BRIGDE MODEL

The 3D model is based on the spatial description of the behaviour of the masonry bridge elements. It is necessary to understand and properly simulate the dynamic and structural properties of the bridge constitutive elements. The mono-dimensional non-linear element, having truncated-pyramid shape, previously described in § *Mono-dimensional non-linear element for 3D modelling*, will be used. The discretization and element assembly procedures arise from these preliminary investigations.

Constitutive elements of the masonry bridge and their structural behaviour

The constitutive portions of a masonry bridge (Albenga [5]), in figure 6, can be briefly identified with: the *vault* (or *arch*) that is the structure supporting the pavement and super-structures; the supporting structures (*pier*, *abutments*) of the vaults; the *foundations*; the apparently non-structural elements, such as *backfill*, *fill* and *impermeable coat,* built above the vaults to create a plane pavement. The fill is sided by two *spandrel walls*, which are built on the external parts of the barrel vault.

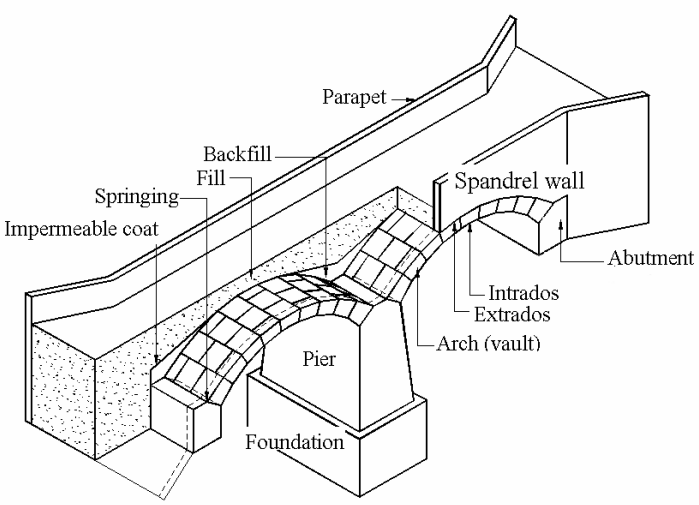

Figure 6. Axonometric section plane of a masonry bridge (Brencich [6]).

The vaulted element is thought so that the radial sections may work prevalently under compressive loading; moreover the behaviour is approximately two-dimensional (the resistant mechanism mainly develops in the longitudinal plane), excluding load redistribution due to the different stiffness of the spandrel walls and the central portion of the vault. Under dead load and vertical load condition, this hypothesis seems to be adequate. This is no more verified in case of seismic event, because of which relevant transversal effects could develop and the vault could behave in a three-dimensional way. We have to simulate both the damage mechanisms in the thickness of the arch (figure 7-a), including crack opening and crushing due to compressive forces, and those involving the whole vault (figure 7-b), connected to crack opening, crushing due to compressive forces, shear forces and sliding in the mortar joints.

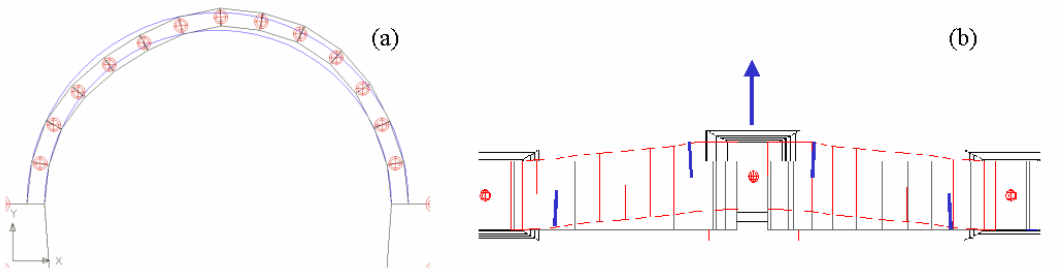

Figure 7. Damage mechanism schematisation: (a) in the arch thickness; (b) in the whole vault (top view).

In the piers, the damage mechanisms connected to the seismic action include crack opening, crushing due to compressive forces, shear forces and sliding in the mortar joints in the transversal direction (along which the pier is generally squatter). The discretization and element assembly procedures (figure 8) arise from these crucial structural and dynamic remarks.

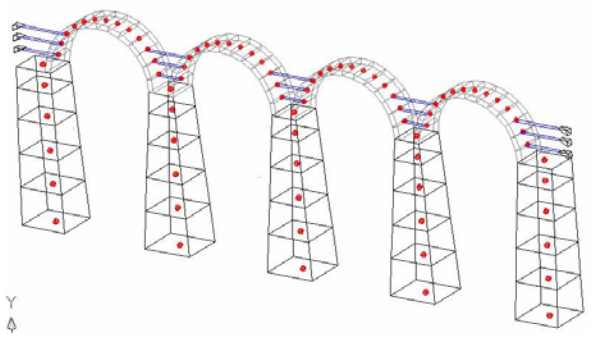

Figure 8. Masonry bridge discretization through mono-dimensional non-linear elements.

By using the mono-dimensional non-linear element (having two nodes) described in figure 3, the masonry bridge can be discretizated in order to better simulate the global structural behaviour. The vault elements are assembled along the circular direction of the vault itself. In the piers and abutments, the elements are arranged along the vertical direction and the pre-defined damage direction, in case of shear and sliding, is the transversal one. The elements have truncated-pyramid shape, in order to mesh in a proper way the masonry piers.

SEISMIC ANALYSIS PROCEDURES

In order to perform non-linear seismic analyses of URM buildings and bridges a set of analysis procedures has been implemented [4]: incremental static (Newton-Raphson) with force or displacement control, 3D pushover analysis with fixed load pattern and 3D time-history dynamic analysis (Newmark integration method; Rayleigh viscous damping), considering uniform or spatially varying motion. The pushover procedure, with an effective algorithm, transforms the problem of pushing a structure maintaining constant ratios between the applied forces into an equivalent incremental static analysis with one d.o.f. displacement response control.

3D Pushover Analysis

The general formulation of the pushover problem can be represented by equations:

$$\begin{bmatrix} \mathbf{K}_{\mathbf{FF}} & \mathbf{k}_{\mathbf{Fm}} & \mathbf{K}_{\mathbf{FC}} \\ \mathbf{k}_{\mathbf{Fm}}^{\mathbf{T}} & k_{mm} & \mathbf{k}_{\mathbf{Cm}}^{\mathbf{T}} \\ \mathbf{K}_{\mathbf{CF}} & \mathbf{k}_{\mathbf{Cm}} & \mathbf{K}_{\mathbf{CC}} \end{bmatrix} \begin{Bmatrix} \mathbf{x}_{\mathbf{F}} \\ x_m \\ \mathbf{x}_{\mathbf{C}} \end{Bmatrix} = \begin{Bmatrix} \lambda \mathbf{f}_{\mathbf{F}} \\ \lambda f_m \\ \mathbf{r}_{\mathbf{C}} \end{Bmatrix}, \tag{12}$$

where m is the control degree of freedom and $\mathbf{f}_F$ is the applied load pattern coefficient vector.

The system of equations can be transformed subtracting the *m-th* row from the first *m-1*, the *i-th* equation then becomes:

$$\left(k_{i1} - \frac{f_i}{f_m} k_{m1}\right) x_1 + \ldots + \left(k_{im} - \frac{f_i}{f_m} k_{mm}\right) x_m + \ldots + \left(k_{in} - \frac{f_i}{f_m} k_{mn}\right) x_n = 0 . \tag{13}$$

The new system of equations, with a modified stiffness matrix,

$$\begin{bmatrix} \tilde{\mathbf{K}}_{\mathbf{FF}} & \tilde{\mathbf{k}}_{\mathbf{Fm}} & \tilde{\mathbf{K}}_{\mathbf{FC}} \\ \mathbf{k}_{\mathbf{Fm}}^{\mathbf{T}} & k_{mm} & \mathbf{k}_{\mathbf{Cm}}^{\mathbf{T}} \\ \mathbf{K}_{\mathbf{CF}} & \mathbf{k}_{\mathbf{Cm}} & \mathbf{K}_{\mathbf{CC}} \end{bmatrix} \begin{Bmatrix} \mathbf{x}_{\mathbf{F}} \\ x_m \\ \mathbf{x}_{\mathbf{C}} \end{Bmatrix} = \begin{Bmatrix} \mathbf{0} \\ \lambda f_m \\ \mathbf{r}_{\mathbf{C}} \end{Bmatrix}, \tag{14}$$

is then equivalent to a displacement control one, in which the *m-th* d.o.f. (x_m) is the imposed one. This formulation can be easily rewritten by introducing the non-linear contribution and in incremental form, in order to be implemented in the non-linear procedure.

Spatially varying dynamic excitation (multiple-support motion)

In case of spatially varying motion (multiple-support), we need to consider the excitation as imposed base motion. The procedure (Resemini [4]) has to be developed in terms of total displacements, because, in order to determine the forces due to non-linear effects, it is not possible to operate in terms of relative displacements. The motion differential equations in case of a discrete linear elastic structural system can be represented in terms of matrices, partitioned in constrained d.o.f. **u** (the sub-matrices have F as subscript) and free d.o.f. **q** (the sub-matrices have C as subscript). Using a time discretization, at the step i+1 the equations are:

$$\begin{bmatrix} \mathbf{M_{FF}} & \mathbf{0} \\ \mathbf{0} & \mathbf{0} \end{bmatrix} \begin{Bmatrix} \ddot{\mathbf{q}}_{\mathbf{i+1}} \\ \ddot{\mathbf{u}}_{\mathbf{i+1}} \end{Bmatrix} + \begin{bmatrix} \mathbf{C_{FF}} & \mathbf{C_{FC}} \\ \mathbf{C_{CF}} & \mathbf{C_{CC}} \end{bmatrix} \begin{Bmatrix} \dot{\mathbf{q}}_{\mathbf{i+1}} \\ \dot{\mathbf{u}}_{\mathbf{i+1}} \end{Bmatrix} + \begin{bmatrix} \mathbf{K_{FF}} & \mathbf{K_{FC}} \\ \mathbf{K_{CF}} & \mathbf{K_{CC}} \end{bmatrix} \begin{Bmatrix} \mathbf{q}_{\mathbf{i+1}} \\ \mathbf{u}_{\mathbf{i+1}} \end{Bmatrix} = \begin{Bmatrix} \mathbf{0} \\ \mathbf{r}_{\mathbf{i+1}} \end{Bmatrix}. \tag{15}$$

In order to obtain the expected value of the displacements **q** at the step i+1, we use Newmark integration method in the incremental formulation. In case of non-linear constitutive model, the calculated elastic displacements, evaluated using the initial stiffness matrix, do not automatically satisfy the balance equation (in terms of total displacements) between the non-linear forces, due to the non-linear constitutive model, and the other actions. We need to develop an iterative procedure to correct the incremental displacement values, in order to converge to a predetermined value.

The first trial value of the incremental displacement $\mathbf{\Delta q_{i+1}}$ is the linear elastic prediction and consequently the displacement is $\mathbf{q_{i+1} = q_i + \Delta q_{i+1}}$. At the step i+1, the non-linear forces $\mathbf{f_F^{non-lin}}$ are evaluated through the total displacement vector $\{\mathbf{q_{i+1}}\ \mathbf{u_{i+1}}\}^{\mathrm{T}}$.

The motion equations related to the free d.o.f. at the i+1 step can be express through the relation:

$$\mathbf{M_{FF}\ddot{q}_{i+1} + C_{FF}\dot{q}_{i+1} + C_{FC}\dot{u}_{i+1} + f_{Fi+1}^{non\text{-}lin}(q_{i+1}, u_{i+1}) = 0}. \tag{16}$$

By introducing:

$$\mathbf{f_{Fi+1}^{earth.} = M_{FF}\ddot{q}_{i+1} + C_{FF}\dot{q}_{i+1} + C_{FC}\dot{u}_{i+1}} \tag{17}$$

$$\mathbf{M_i} = \mathbf{M_{FF}} \frac{1}{\beta \Delta t^2} + \mathbf{C_{FF}} \frac{\gamma}{\beta \Delta t} \tag{18}$$

$$\mathbf{M_1} = -\mathbf{M_{FF}} \frac{1}{\beta \Delta t} - \mathbf{C_{FF}} \frac{\gamma}{\beta} \tag{19}$$

$$\mathbf{M_2} = -\mathbf{M_{FF}} \frac{1}{2\beta} + \mathbf{C_{FF}} \left(1 - \frac{\gamma}{2\beta} \right) \cdot \Delta t\ , \tag{20}$$

where β and γ are the Newmark coefficients and substituting these expressions in Eq.(16), we may derive the following relation:

$$\mathbf{f_{i+1}^{earth.} = f_i^{earth.} + M_i \Delta q_{i+1} + M_1 \dot{q}_i + M_2 \ddot{q}_i + C_{FC} \Delta \dot{u}_{i+1}}. \tag{21}$$

The balance equations between the involved forces have the following form:

$$\mathbf{f_{Fi+1}^{earth.} + f_{Fi+1}^{non\text{-}lin} = 0}. \tag{22}$$

Through Newton-Raphson convergence procedure, we can correct, using the modified stiffness matrix $\tilde{\mathbf{K}}_{\mathbf{FF}} = \frac{1}{\beta \Delta t^2}\mathbf{M}_{\mathbf{FF}} + \frac{\gamma}{\beta \Delta t^2}\mathbf{C}_{\mathbf{FF}} + \mathbf{K}_{\mathbf{FF}}$, the predicted value of the incremental displacement $\Delta\tilde{\mathbf{q}}_{\mathbf{i+1}}$, substituting in the relation:

$$\Delta\tilde{\mathbf{q}}_{\mathbf{i+1}} = \tilde{\mathbf{K}}_{\mathbf{FF}}^{-1} \cdot (\mathbf{f}_{\mathbf{Fi+1}}^{earth.} + \mathbf{f}_{\mathbf{Fi+1}}^{non\text{-}lin}) \tag{23}$$

The total displacement at the step i+1 is evaluated using the new value of $\Delta\tilde{\mathbf{q}}_{\mathbf{i+1}}$, and the procedure iterates until convergence.

EXPERIMENTAL TESTING SIMULATION

Pavia house cyclic tests

In order to demonstrate the reliability of the model, a numerical simulation of experimental testing on a full-scale masonry building accomplished in the Laboratory of the University of Pavia (Magenes [7]) is here presented.

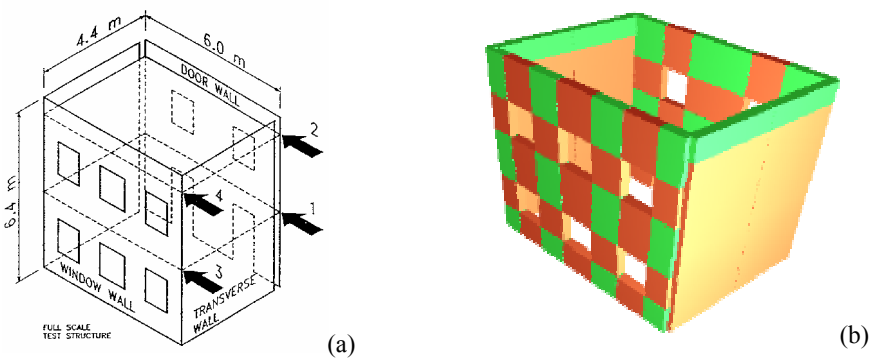

Figure 9. (a) Scheme of the test; (b) 3-dimensional view of the macro-element model.

As shown in figure 9-a, the experimental tests have been carried out on two separated structural systems: the isolated "door" wall and the "window" wall connected to the two transverse walls. The numerical simulation has then performed by cyclic analysis of two different macro-element models (figure 10) with the same mechanical characteristics: the window wall system has been modelled using 12 nodes and 21 macro-elements, the door wall 9 nodes and 10 macro-elements.

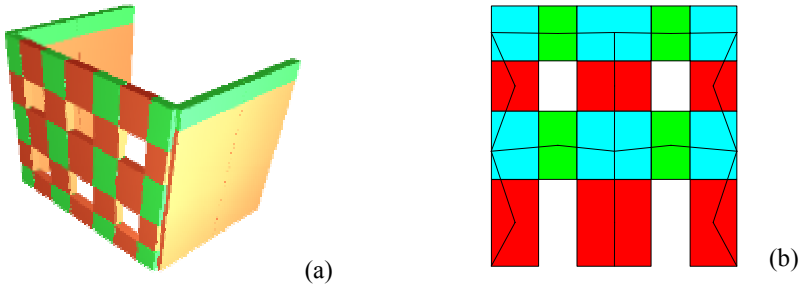

Figure 10. (a) 3D model of window and transverse walls; (b) 2D model of door wall.

The numerical and experimental results are in good accordance, both in terms of cyclic base shear-second floor displacement curves (figure 11) and damage localization at the different load steps. The model can well represent the real collapse mechanism and reproduce correct levels of strength and hysteretic energy dissipation.

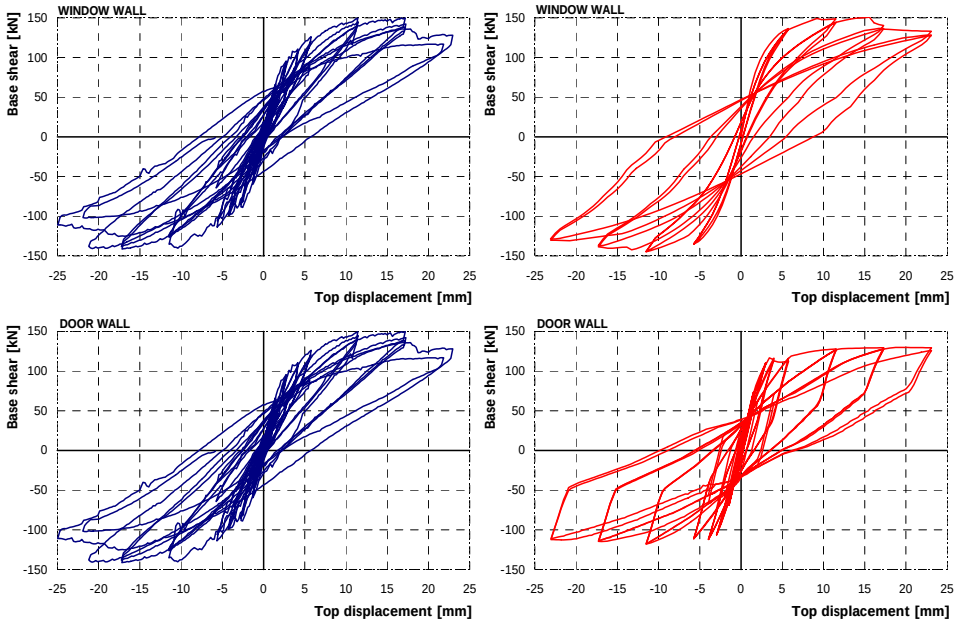

Figure 11. Comparison of experimental (left) and numerical (right) results.

CASE STUDIES

The Castelnuovo Belbo Hall (Piedmont) damaged by the 2000 Monferrato earthquake

A complete 3D macro-element model (see figure 12) of the Hall of Castelnuovo Belbo village, in Piedmont, Northern Italy, has been used in order to simulate the building seismic response and the damage pattern surveyed after August 21st 2000 Monferrato earthquake (M_d=4.6).

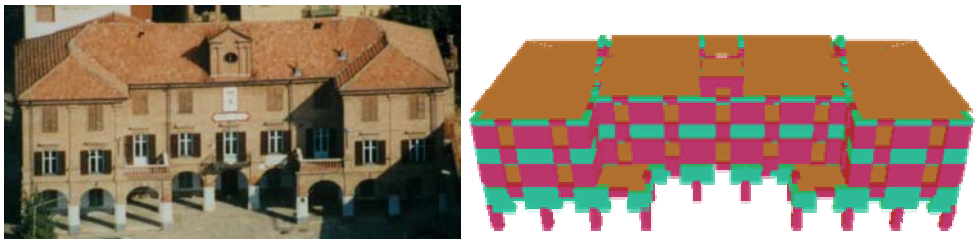

Figure 12. Aerial view of the building and perspective view of TREMURI 3D model.

By means of a non-linear time-history analysis, the global seismic response has been investigated: an artificial accelerogram scaled to the maximum recorded PGA during the seismic event (0.14 g) has been used as input.

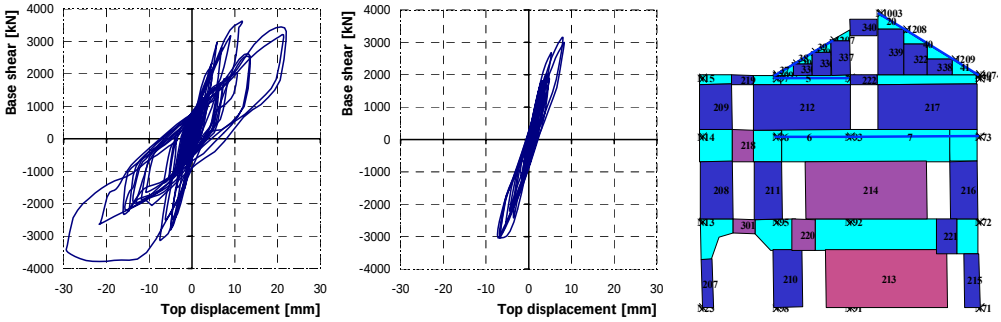

Figure 13. Dynamic force-displacement response [0.35 g and 0.14 g] and damage pattern in a wall.

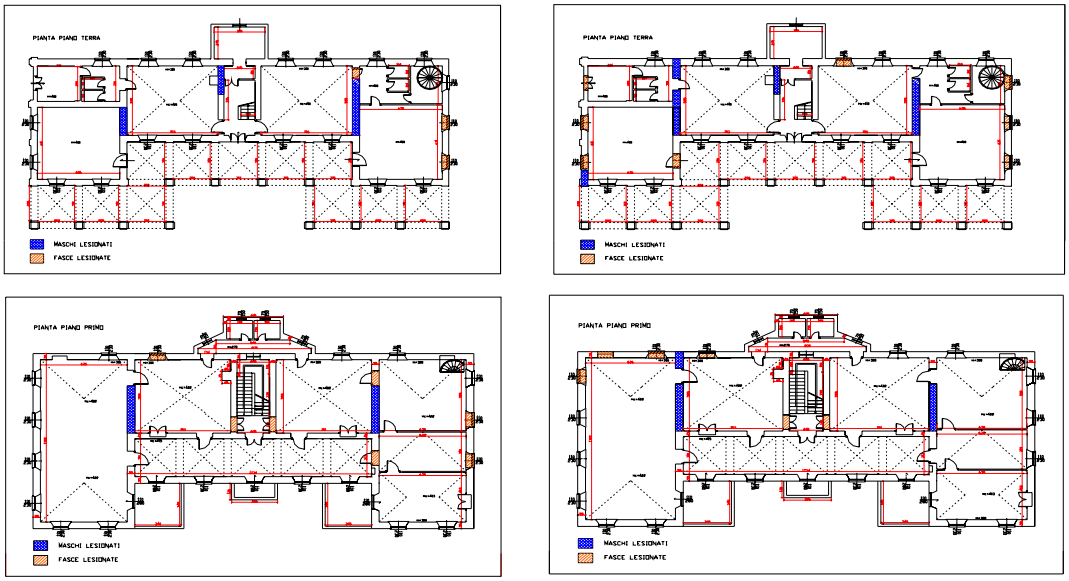

(a) (b)

Figure 14. Damage pattern simulation: (a) surveyed and (b) simulated damage.

Giuncugnano Hall, Tuscany

The Hall of the Giuncugnano village in Tuscany is an instrumented building included in the Structure Seismic Observatory (OSS) program of the Italian National Seismic Survey (SSN).

This URM building, like several others all around Italy, now hosts a set of accelerometers which permanently monitor its dynamic response.

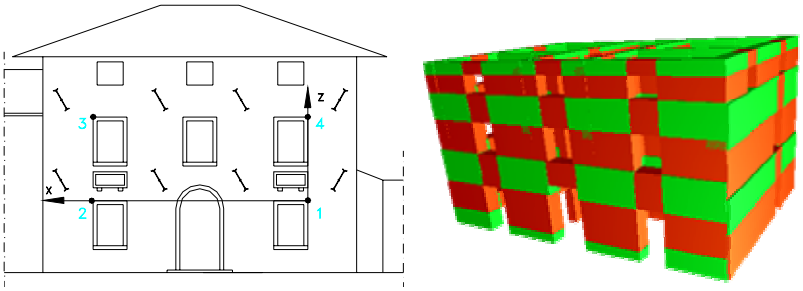

Figure 15. Front view and 3D building model of the Giuncugnano Hall.

In-situ and laboratory tests have been performed in order to obtain a good characterisation of the structural behaviour both for linear and non-linear response. Modal tests allowed good data for dynamic identification of the 3D macro-element model: numerical modal analysis results, accordingly to experimental ones, are shown in figure 16.

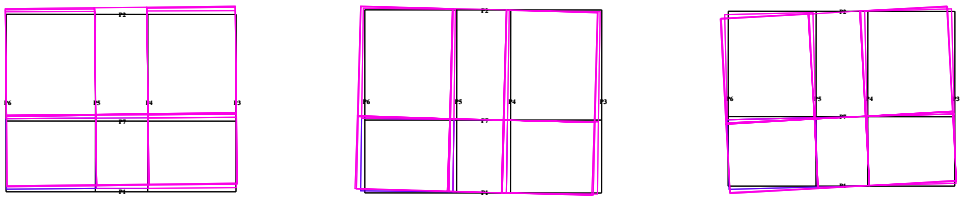

$T_1 = 0.139$ $T_2 = 0.119$ $T_3 = 0.105$

Figure 16. Modal analysis results.

Non-linear pushover analyses have been performed on the identified model, in order to detect on the capacity curve the damage limit states and the expected seismic performance.

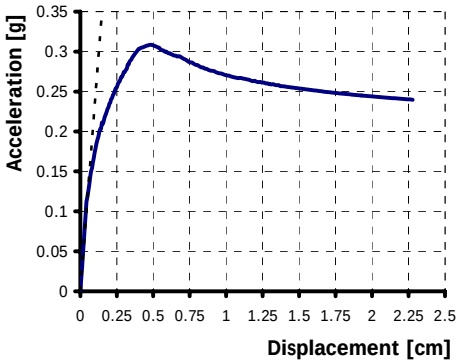

Figure 17. Capacity curve obtained by the pushover analysis.

Dynamic analysis of the Acquasanta Viaduct (Genoa, Italy)

In a site with a particular geo-morphological environment, amplification effects may lead to a 3D spatially varying seismic action. In case of masonry bridges having multiple supports (piers), these can be founded in soil with different mechanical characteristics and on steep slopes. The seismic excitation may be modified (in intensity and phase) by stratigraphic and/or morphological conditions, and so each pier could have a different imposed motion. These aspects may be very significant to the masonry bridge structural behaviour and damage state. The Acquasanta Viaduct (figure 18), in the Northern Italy railway network, is a monumental masonry structure (11 arcades of 18.5 m span, maximum height of the pier 50 m). The geo-morphological site conditions are interesting, because the central piers are founded in soil characterized by poor mechanical properties.

Figure 18. Acquasanta Viaduct (Genoa, Italy); west side on the right.

This material derives from the schist alteration, due to a tectonic contact between two different rock materials; the depth of this altered soil (derived by geophysical tests) is remarkable. In order to obtain a prediction of the site effects, several simulations, using a spectral-element code (TRISEE [8]), were performed. In this way, the time histories in terms of total displacement (a different one in correspondence of each pier) were obtained; these were used as input motion in the structural non-linear analyses. The vertical component of motion seems to be pretty amplified from on side to the other: in correspondence of the western piers, the amplification is higher. On this side, the harmonic content of the horizontal component seems modified by the site effects. The earthquakes used in the simulation were recorded in high-seismicity areas in Southern Italy (where masonry bridges are also frequent on the railway network). The results of the dynamic analyses in case of multiple-support motion in the longitudinal plane of the bridge (Resemini [4]) are presented. The non-linear structural model was subjected to an excitation in the horizontal and vertical directions. The peak acceleration corresponding to

the time histories is quite low (0.05 g), in order to observe the initial effects of the damage activation in the dynamic response, but not to be in a strong non-linear phase (in which the differences between the two motion types may be not clearly recognizable). The comparison between uniform (the input is the time history obtained in correspondence of an eastern pier) and spatially varying excitation was studied. In figures 19-20 are represented the time histories of the horizontal and vertical displacement in some significant points of the bridge.

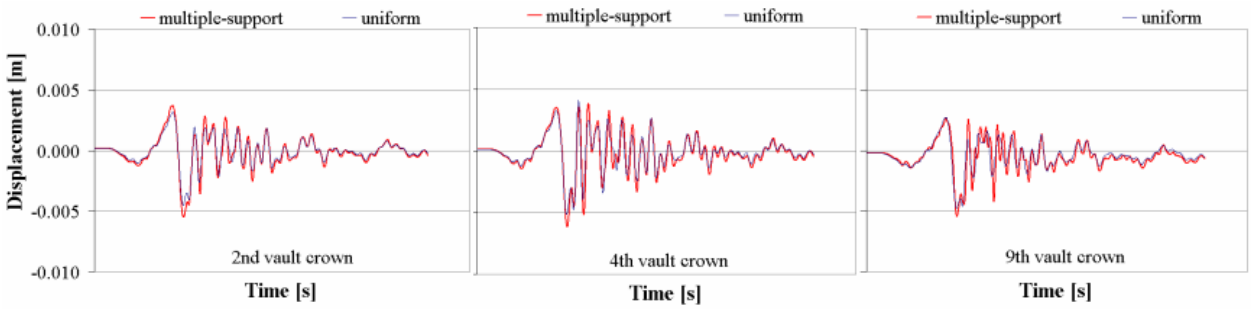

Figure 19. Time histories of the horizontal displacement (time window 0-15 s): comparison between uniform and spatially varying excitation in crown of the vaults (numbered from east to west).

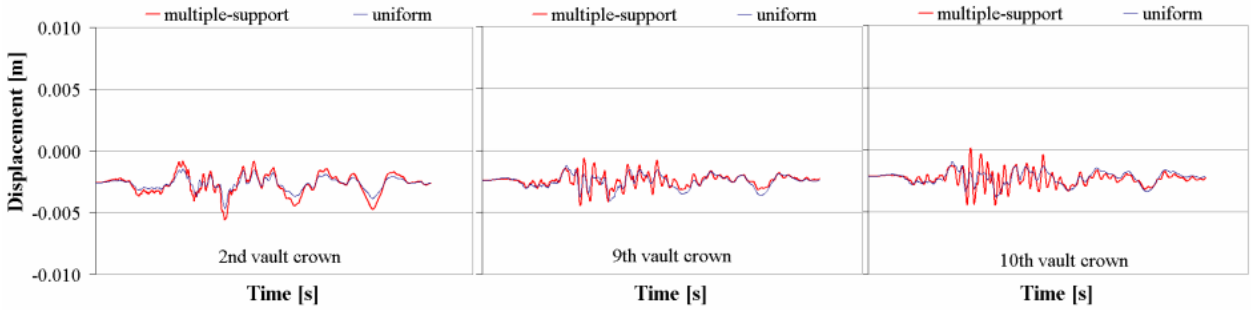

Figure 20. Time histories of the vertical displacement (time window 0-15 s): comparison between uniform and spatially varying excitation in crown of the vaults (numbered from east to west).

Analysing this data, we can notice that, in case of multiple-support motion, the structural response is amplified, especially in the western part of the bridge (in which even the input motion is different from the one in the uniform case). These intensity amplifications are particularly evident in the vertical component of the displacement. The multiple-support excitation influences significantly even the eastern part of the structure, and this (being the input motion the same in the two cases) can be explained only through interaction effects with the other parts of the bridge (absent in case of the uniform motion).

In order to highlight the damage state connected to the progressive partialization in portion of the structure, some analyses using uniform and spatially varying excitation and increasing peak acceleration (0.01g, 0.02g, 0.03g and 0.04g) were developed; the acceleration is quite low, so the initial phase of non-linearity can be observed.

The structural damage is identified through a global parameter ε, that takes into account the partialization level in each element of the model and in each step of the analysis. The behaviour of the global parameter ε is shown in figure 21.

We can notice how the input motion characteristics influence the vulnerability and seismic response of this masonry arch bridge; the difference in percentage of the global parameter ε is case of the two kinds of excitation (uniform and multiple-support motion) becomes higher as the peak acceleration increases.

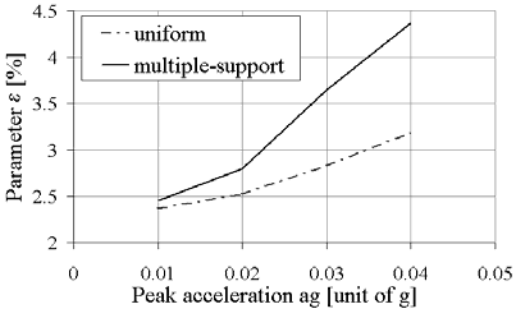

Figure 21. Difference in percentage of the global parameter ε as the peak acceleration increases (uniform and multiple-support motion).

CONCLUSIONS

As shown in the paper, the non-linear macro-element modelling of 3-dimensional URM buildings and bridges supplies reliable results in comparison with experimental data and permits to model effectively different typologies of real masonry structures, too. Its seismic analysis capabilities make the TREMURI program a valid tool both for research activity, especially regarding ancient masonry buildings, and engineering practice. The macro-element model permits to perform reliable non-linear seismic analyses of wide masonry structures with a limited number of d.o.f. and relatively short analysis time using common PC technology. Modern performance-based seismic engineering requires this kind of easy-to-use tools for both capacity assessment and direct time-history response evaluation.
Further development of the TREMURI program with the introduction of other analysis options such as the introduction of adaptive pushover analysis capability and new verification procedures are foreseen.

AKNOWLEDGEMENT

Authors are pleased to thank Prof. Guido Magenes, University of Pavia, who kindly provided experimental data.

REFERENCES

1. Gambarotta L., Lagomarsino S., 1996, "On dynamic response of masonry panels", in Gambarotta L. (ed.) Proc. of the National Conference "La meccanica delle murature tra teoria e progetto", Messina, (in italian).
2. Gambarotta, L., Lagomarsino, S., 1997, "Damage models for the seismic response of brick masonry shear walls, Part II: the continuum model and its applications", Earth. Engineering and Structural Dynamics, **26.**
3. Penna A., 2002, "A macro-element procedure for the non-linear dynamic analysis of masonry buildings", Ph.D. Dissertation (in italian), Politecnico di Milano, Italy.
4. Resemini S., 2003, "Seismic vulnerability of masonry arch bridges", Ph.D. Dissertation (in italian), University of Genoa, Italy.
5. Albenga, G., "The bridges", UTET, Turin, 1958.
6. Brencich, A., De Francesco, U., Gambarotta L., Lagomarsino S., Resemini S., Sereno A., 2001, Technical report "Methodological study and software on the load bearing capacity of masonry arch bridges", Contract University of Genoa-RFI (National Railway Authority) (in italian).
7. Magenes G., Calvi G.M., 1997, "In-plane seismic response of brick masonry walls", Earthquake Engineering and Structural Dynamics, 26.
8. TRISEE, 1998, "3D Site Effects and Soil-Foundation Interaction in Earthquake and Vibration Risk Evaluation", Technical Report, Environment and Climate Program, March 1998.
9. Galasco, A., Lagomarsino, S. and Penna, A., 2002, TREMURI Program: Seismic Analyser of 3D Masonry Buildings, University of Genoa.